Journal of Molecular Structure 976 (2010) 414–418

Contents lists available at ScienceDirect

Journal of Molecular Structure

journal homepage: www.elsevier.com/locate/molstruc

Triplet quantum chain process in the photoisomerization of 9-*cis* retinal as revealed by nanosecond time-resolved infrared spectroscopy

Tetsuro Yuzawa [a], Hiro-o Hamaguchi [a,b,*]

[a] Department of Chemistry, School of Science, The University of Tokyo, 7-3-1 Hongo, Bunkyo-ku, Tokyo 113-0033, Japan
[b] Institute of Molecular Science and Department of Applied Chemistry, National Chiao Tung University, 1001 Ta Hsueh Road, Hsinchu 300, Taiwan

ARTICLE INFO

Article history:
Received 1 March 2010
Received in revised form 20 April 2010
Accepted 20 April 2010
Available online 28 April 2010

Keywords:
Triplet quantum chain
Photoisomerization
9-*Cis* retinal
Nanosecond time-resolved infrared spectroscopy
Photodynamics

ABSTRACT

The mechanism of the photoisomerization of 9-*cis* retinal has been studied by nanosecond time-resolved infrared spectroscopy. A cyclohexane solution of 9-*cis* retinal was photoexcited at 349 nm and the subsequent photodynamics were traced. A singular value decomposition (SVD) analysis of the time-resolved infrared data shows that there are two distinct isomerization pathways. One is the triplet pathway that takes place in the picosecond time regime from 9-*cis* to all-*trans*. The other involves the energy transfer between the all-*trans* triplet state and the 9-*cis* ground state with the resultant 9-*cis* triplet state subsequently reproducing the all-*trans* by fast isomerization on the triplet potential surface. This quantum chain process occurs in the microsecond time regime.

1. Introduction

Retinal has four C=C double bonds that give rise to the four mono-*cis* isomers, the 7-*cis*, 9-*cis*, 11-*cis* and 13-*cis* forms. These isomers undergo *cis*–*trans* isomerization upon photoexcitation. Photoisomerization of retinyl chromophores has been extensively studied in relation to their functions as the photo-receptors in retinoid proteins like rhodopsin and bacteriorhodopsin [1]. Photoisomerization of the retinal molecule itself is also of considerable interest as a prototype unimolecular chemical reaction. A characteristic feature is known for the photoisomerization of retinal in organic solvents. The photoisomerization efficiency is not symmetrical with respect to *cis* and *trans*; the quantum yield of photoisomerization is much higher in the *cis* to *trans* direction than in the *trans* to *cis* [2–4]. This asymmetry is not found for many of ethylene derivatives in which the photoisomerization efficiency is similar for the *trans* to *cis* and the *cis* to *trans* directions [5].

The origin of this asymmetry in the photoisomerization of retinal was elucidated with time-resolved spectroscopies. Transient Raman spectroscopy first showed that the photoexcitation of the 7-*cis*, 9-*cis*, 11-*cis* isomers generated an identical transient Raman spectrum that was assigned to the all-*trans* triplet state. It was considered that isomerization of 7-*cis* (or 9-*cis*, 11-*cis*-) to all-*trans* took place on the lowest triplet potential surface (one-way photoisomerization) [6]. Picosecond time-resolved absorption spectroscopy then showed that the 9-*cis* T_1 species isomerizes to all-*trans* in sub-nanosecond time regime [7]. Picosecond 2D-CARS and femtosecond absorption experiments clarified that the 9-*cis* to all-*trans* conversion time was 880 ps on the triplet potential surface [8,9]. The photoisomerization of all-*trans* retinal was studied with nanosecond time-resolved infrared spectroscopy [10]. It was found that, immediately after photoexcitation, the all-*trans* T_1 state was generated within the time resolution of the system and decayed to the all-*trans* S_0 state with no isomerization. It was also found that a very fast isomerization pathway existed from the all-*trans* to 13-*cis*/9-*cis* via the excited singlet state. Femtosecond ultraviolet–visible absorption spectroscopy clearly showed that this all-*trans* to mono-*cis* photoisomerization took place via the S_2 state [11,12]. These time-resolved spectroscopic studies have clearly showed that the *cis* to *trans* photoisomerization of retinal proceeds predominantly on the excited triplet potential surface but that the *trans* to *cis* proceeds via the second excited singlet state. The *cis*–*trans* asymmetry originates from the different pathways of the photoisomerization.

Another mechanism that favors the *cis* to *trans* isomerization of retinal is the triplet quantum chain process, in which the *trans* excited triplet state generated from the *cis* by the one-way isomerization reacts with the ground state *cis* molecule to generate the *cis* excited triplet state and the *trans* ground state. The *cis* excited triplet state thus formed further isomerizes on the triplet potential

* Corresponding author at: Department of Chemistry, School of Science, The University of Tokyo, 7-3-1 Hongo, Bunkyo-ku, Tokyo 113-0033, Japan.
E-mail address: hhama@chem.s.u-tokyo.ac.jp (H. Hamaguchi).

0022-2860/$ - see front matter © 2010 Elsevier B.V. All rights reserved.
doi:10.1016/j.molstruc.2010.04.031

surface to the *trans*. The possibility of this triplet quantum chain process has been pointed out from the concentration dependence of the quantum yield of photoisomerization [4,13,14]. In the present paper, we use time-resolved infrared spectroscopy to directly monitor the triplet quantum chain process in the photoisomerization of 9-*cis* retinal.

2. Experimental

The experimental arrangements for AC-coupled nanosecond time-resolved infrared spectroscopy with a dispersive spectrometer (JASCO TRIR-1000) have been described in detail in previous papers [15–17]. A photovoltaic MCT detector (Kolmar Technologies, Inc. KV103-1-A-1-SMA) was used for fast infrared detection. The time resolution was about 50 ns. Signals from the MCT detector are first amplified with a preamplifier and then averaged on a digital oscilloscope (Tektronix DSA602). A sampling rate of data acquisition was every 40 ns for the experiments described here. The third harmonic of a cw Q-switched Nd:YLF Laser (Spectra Physics TFR, 5 ns pulse width, 190 Hz repetition rate, 30 mJ at 349 nm) was used for photoexcitation. Infrared absorption spectra were obtained at intervals of 4 cm^{-1} with a spectral resolution of 16 cm^{-1}. A cyclohexane solution of retinal was circulated with peristaltic pump to eliminate the influence of the photoisomerization products. A flowing sample cell with two BaF_2 windows was used. Solutions were bubbled with argon gas during the measurements in order to eliminate the effect of oxygen. Samples of all-*trans*-retinal and 9-*cis*-retinal were purchased from Sigma and used as received. Cyclohexane was purchased from Wako Pure Chemical Industry, Ltd. and used without further purification. All measurements were carried out at room temperature.

3. Results and discussion

3.1. Time-resolved infrared difference spectra

Time-resolved infrared difference spectra of photoexcited 9-*cis* retinal in cyclohexane (3.5 mM) are shown in Fig. 1. These difference spectra, which correspond to the light-on minus light-off signal, were obtained directly with the AC-coupled method [15–17]. Spectra were averaged over the delay time ranges shown in the caption. The wavenumber regions around 1450 cm^{-1} and 1030 cm^{-1} were blocked by the strong absorption bands of cyclohexane. Negative peaks at 1670, 1588, 964 cm^{-1} show the depletion of 9-*cis* retinal in the ground state by the photoexcitation. Positive peaks at 1602, 1552, 1184 and 940 cm^{-1} represent the production of transient species. After the delay of 18 μs (Fig. 1m) the observed difference spectrum shows no further temporal change. The difference spectrum after 18 μs is identical with the difference spectrum between the all-*trans* isomer and the 9-*cis* isomer in the ground state. The negative peaks at 1592, 1144, and 960 cm^{-1} are ascribed to 9-*cis* S_0. The positive peaks at 1570, 1164, 1130, and 972 cm^{-1} are ascribed to all-*trans* S_0. It is thus indicated that the photoexcitation of 9-*cis* retinal in cyclohexane solution causes the photoisomerization to the all-*trans* isomer.

Temporal profiles of the signal observed at four different wavenumbers are shown in Fig. 2. The best fit of those curves with the single exponential function convoluted with the instrumental response are shown as solid lines in Fig. 2. A global fitting analysis of these curves gives a single time constant of 5 μs. The positive peaks at 1184 cm^{-1} (Fig. 2c) and 1600 cm^{-1} (Fig. 2d) are assigned to the all-*trans* triplet state [10]. They show instantaneous rise and along with decay with the time constant of 5 μs. The response of the present time-resolved infrared apparatus is not sufficient to resolve the fast rise (880 ps) of the all-*trans* triplet state from the 9-*cis*.

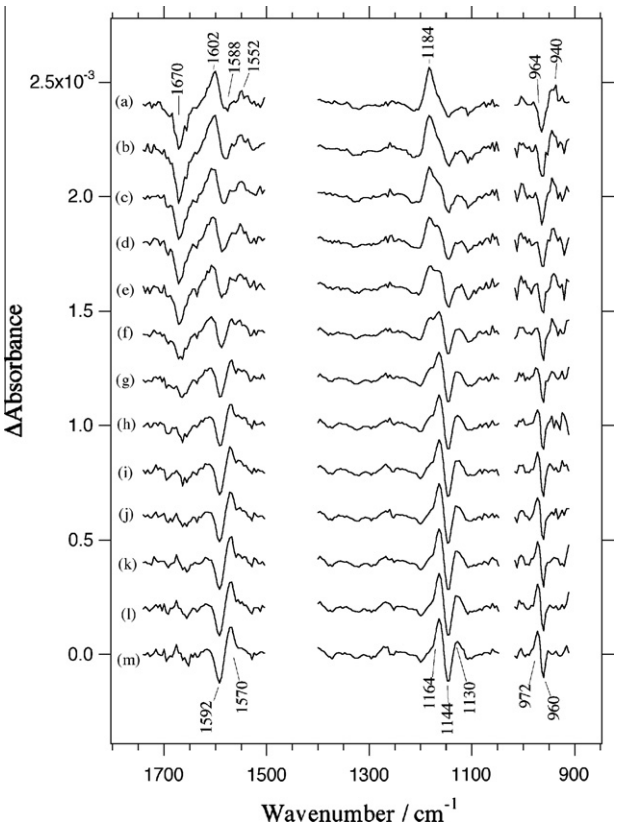

Fig. 1. Time-resolved infrared difference spectra of photoexcited 9-*cis* retinal in cyclohexane. (a) 0 ns–0.4 μs, (b) 0.4 μs–0.8 μs, (c) 0.8 μs–1.2 μs, (d) 1.2 μs–1.6 μs, (e) 1.6 μs–2 μs, (f) 2 μs–4 μs, (g) 4 μs–6 μs, (h) 6 μs–8 μs, (i) 8 μs–10 μs, (j) 10 μs–12 μs, (k) 12 μs–14 μs, (l) 14 μs–16 μs and (m) 16 μs–18 μs.

The negative band at 1144 cm^{-1} (Fig. 2a) represents the depletion of 9-*cis* retinal in the ground state. Neither all-*trans* T_1 nor all-*trans* S_0 show a band at 1144 cm^{-1}. The temporal profiles of this band observed for three different concentrations are shown in Fig. 3. The signal can be separated into two temporal components. One is the instantaneous decrease of the signal (denoted as I_1 in the trace Fig. 3a), which is ascribed to the instantaneous depletion of 9-*cis* S_0 by the photoexcitation. The other is denoted as I_2 in the trace Fig. 3b, which is ascribed to the delayed depletion of 9-*cis* S_0 in the microsecond time regime. The second component suggests that there is a pathway that consumes the ground state of 9-*cis* retinal in the microsecond regime. The contribution of the I_2 component to the whole amount of the 9-*cis* S_0 depletion depends on the concentration of retinal. At a high concentration (Fig. 3a, 3.2 mM), the amplitude of I_2 is comparable to that of I_1. At a low concentration (Fig. 3c, 0.28 mM), the amplitude of I_2 becomes negligible. The intensity of the 1144 cm^{-1} band decreases at the rate of 5 μs, which is the same as that of the decay of all-*trans* T_1. This fact indicates that an interaction between the 9-*cis* S_0 and all-*trans* T_1 is involved in the photoprocess.

3.2. SVD analysis

The time-resolved infrared difference spectra shown in Fig. 1 have been analyzed with the singular value decomposition (SVD) method. The decomposed spectral and temporal components obtained are shown in Fig. 4 for the largest four singular values, which are 0.00952, 0.00463, 0.00170, 0.00166. It is obvious from

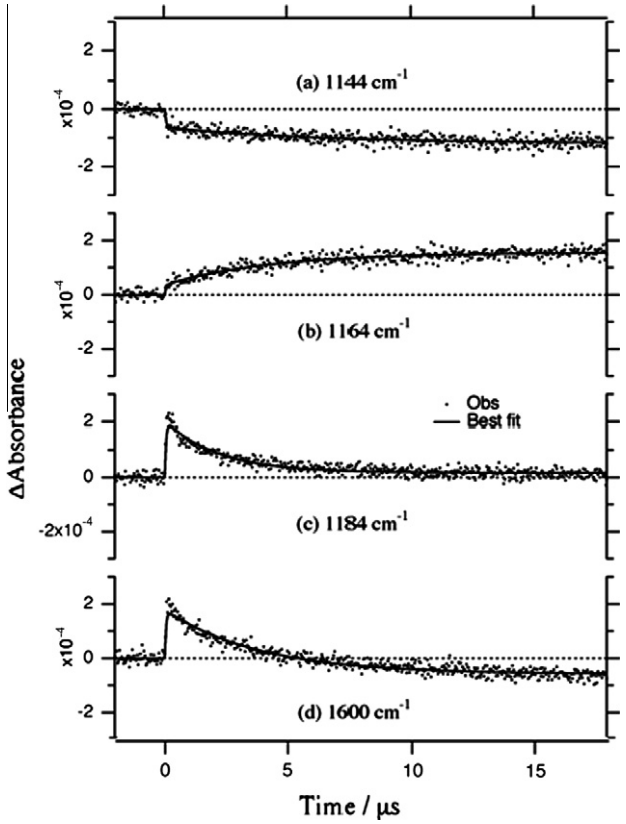

Fig. 2. Temporal profiles observed at 1144 cm^{-1} (a), 1164 cm^{-1} (b), 1184 cm^{-1} (c) and 1600 cm^{-1} (d). The dotted lines show the observed signals and the solid lines show best fits with exponential functions.

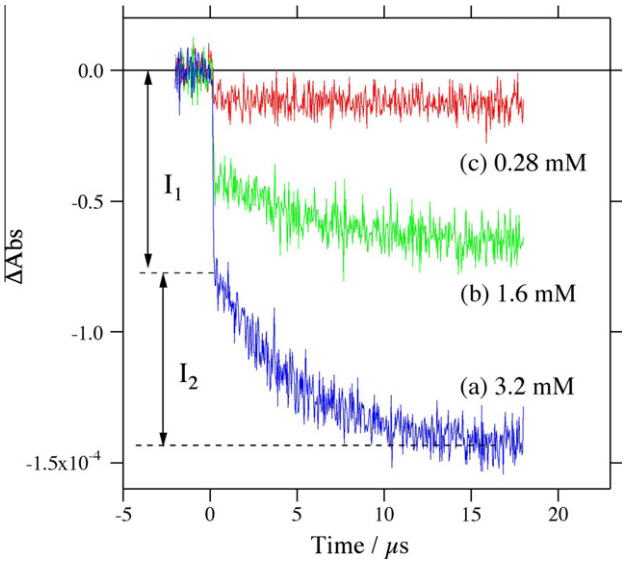

Fig. 3. Decay curves observed at 1144 cm^{-1} for three different concentrations of retinal. (a) 3.2×10^{-3} M, (b) 1.6×10^{-3} M, (c) 2.8×10^{-4} M.

the figure that two of the four components (Fig. 4a and b for the spectrum, and Fig. 4e and f for the temporal profile) are dominant and that the third and the fourth components contain no meaningful features. Thus, the third and fourth components are discarded in the following analysis.

Because SVD itself is a pure mathematical operation, only appropriate linear combinations of the components are physically

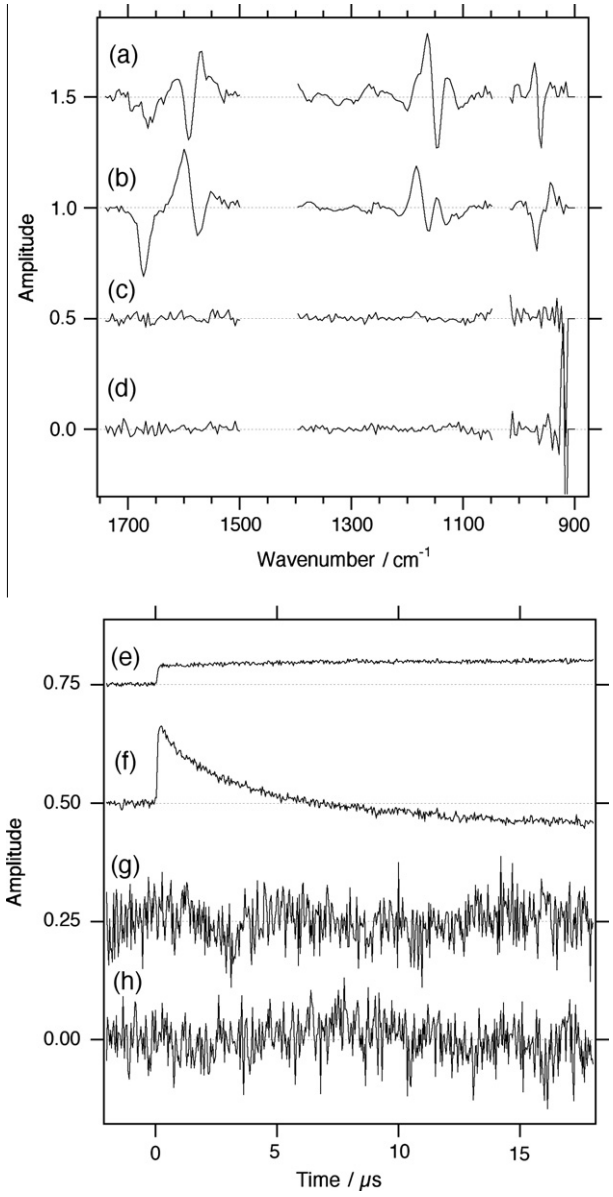

Fig. 4. Spectral components (a, b, c, d) and temporal components (e, f, g, h) obtained by the SVD analysis. The components correspond to the largest four singular values are shown in the descending order from the top to bottom.

meaningful. In general, a time-resolved spectroscopic data matrix A consisting of N independent spectral components is written as a linear combination of the product of $\mathbf{u}_k$ and $\boldsymbol{v}_k$, where $\mathbf{u}_k$ is a column vector representing a temporal profile and $\boldsymbol{v}_k$ is a row vector representing a spectral component.

$$\mathbf{A} = \sum_{k=1}^{N} w_k \mathbf{u}_k \cdot \boldsymbol{v}_k \tag{1}$$

Here, $\mathbf{u}_k$ and $\boldsymbol{v}_k$ are normalized and the coefficient w_k denotes the singular value. The operator dot represents the outer product of two vectors. If only two of the decomposed components are dominant and the rest of the components are discarded as noise, the time-resolved infrared data matrix A is approximated as:

$$\mathbf{A} \approx w_1 \times \mathbf{u}_1 \cdot \mathbf{v}_1 + w_2 \times \mathbf{u}_2 \cdot \mathbf{v}_2. \tag{2}$$

There are two possible photoisomerization pathways for photo-excited 9-*cis* retinal. One is the known pathway that proceeds on the excited triplet potential; the excited triplet state of 9-*cis* retinal

isomerizes to the all-*trans* isomer with the time constant of 880 ps [8]. The other pathway is via the excited singlet state. The excited singlet state of 9-*cis* retinal might well isomerize to the excited singlet state of all-*trans* isomer, which subsequently relaxes either to all-*trans* T_1 or to all-*trans* S_0 in the picosecond regime [9]. The time resolution of the present experiment is about 50 ns. Consequently, the first pathway via the triplet manifold is expected to give an instantaneous rise of the all-*trans* T_1 signal followed by a decay in the microsecond time regime. The latter pathway is expected to give an instantaneous rise of the signal of all-*trans* T_1 and/or all-*trans* S_0. The temporal behavior of the signal at 1144 cm^{-1} indicates that the depletion of 9-*cis* S_0 proceeds also with the time constant of 5 μs and this process has to be included in the photodynamics. Thus, the following five kinetics are assumed to describe the temporal behavior of the time-resolved spectra. (1) The instantaneous rise of all-*trans* T_1 and its decay with the time constant of 5 μs. (2) The instantaneous rise of all-*trans* T_1 and all-*trans* S_0. (3) The instantaneous depletion of 9-*cis* S_0 by the photoexcitation. (4) The growth of all-*trans* S_0 with the time constant of 5 μs. (5) The depletion 9-*cis* S_0 with the time constant of 5 μs. The combination of these five kinetics is expected to reproduce the time-resolved infrared data. Here we define the following temporal functions.

$$\mathrm{Exp}_{-} \equiv \mathrm{Exp}_{-}(t) \equiv \begin{cases} 0 & (t < 0) \\ \exp(-k_0 t) & (t \geqslant 0) \end{cases}$$
$$\mathrm{Exp}_{+} \equiv \mathrm{Exp}_{+}(t) \equiv \begin{cases} 0 & (t < 0) \\ 1 - \exp(-k_0 t) & (t \geqslant 0) \end{cases} \quad (3)$$
$$\mathrm{Step} \equiv \mathrm{Step}(t) \equiv \begin{cases} 0 & (t < 0) \\ 1 & (t \geqslant 0) \end{cases}$$

The photoexcitation corresponds to $t = 0$. The function Exp_{-} describes an exponential decay with a rate constant of k_0, the Exp_{+} function describes an exponential growth with the same rate constant of k_0, and the Step function describes an instantaneous rise (positive) or depletion (negative). Note that the rate constant k_0 corresponds to the observed time constant of 5 μs. The Exp_{-} function represents the behavior of all-*trans* T_1 signal in the kinetics (1). The Exp_{+} function represents the growth of the signal with the time constant of 5 μs (kinetics (4) and (5)). The Step function represents the instantaneous signal change (kinetics (2) and (3)). Based on the five kinetic schemes, A is represented as follows.

$$\mathbf{A} = a1 \times \mathbf{u}_{\mathrm{exp}-} \cdot \mathbf{v}_{AT-T} + a_2 \times \mathbf{u}_{\mathrm{step}} \cdot \mathbf{v}_{AT-G} + a_3 \times \mathbf{u}_{\mathrm{step}} \cdot \mathbf{v}_{9C-G} + a_4 \times \mathbf{u}_{\mathrm{exp}+} \cdot \mathbf{v}_{AT-G} + a_5 \times \mathbf{u}_{\mathrm{exp}+} \cdot \mathbf{v}_{9C-G} \quad (4)$$

Here, $\mathbf{v}_{AT-T}$, $\mathbf{v}_{AT-G}$ and $\mathbf{v}_{9C-G}$ represent the spectra of all-*trans* T_1, all-*trans* S_0, and 9-*cis* S_0, respectively, and $\mathbf{u}_{\mathrm{exp}-}$, $\mathbf{u}_{\mathrm{exp}+}$ and $\mathbf{u}_{\mathrm{step}}$ represent the Exp_{-} function, the Exp_{+} function, and the Step function, respectively. The coefficients a_1, a_2, a_3, a_4 and a_5 represent the contributions of the five terms. The Step function is given as a linear combination of the Exp_{-} and Exp_{+} functions as: $\mathrm{Step} = \mathrm{Exp}_{-} + \mathrm{Exp}_{+}$. Substituting the Step function with $\mathrm{Exp}_{+} + \mathrm{Exp}_{-}$, **A** is represented as follows.

$$\mathbf{A} = \mathbf{u}_{\mathrm{exp}-} \cdot (a_1 \times \mathbf{v}_{AT-T} + a_2 \times \mathbf{v}_{AT-G} + a_3 \times \mathbf{v}_{9C-G}) + \mathbf{u}_{\mathrm{exp}+} \cdot (a_2 \times \mathbf{v}_{AT-G} + a_3 \times \mathbf{v}_{9C-G} + a_4 \times \mathbf{v}_{AT-G} + a_5 \times \mathbf{v}_{9C-G}) \quad (5)$$

Eq. (5) indicates that **A** can be decomposed into two spectral components that have the temporal behaviors described with $\mathbf{u}_{\mathrm{exp}-}$ and $\mathbf{u}_{\mathrm{exp}+}$. Appropriate linear combinations of the two SVD temporal components (Fig. 4e and f) should then make $\mathbf{u}_{\mathrm{exp}-}$ and $\mathbf{u}_{\mathrm{exp}+}$. The coefficients of these appropriate linear combinations were obtained by a least-squares fitting of curves Fig. 4e and f to $\mathbf{u}_{\mathrm{exp}-}$ and $\mathbf{u}_{\mathrm{exp}+}$. The spectral and temporal components thus determined are shown in Fig. 5. The observed time-resolved infrared spectra were very well reconstructed from these SVD spectral and temporal components.

We now examine the physical meanings of the retrieved SVD components in Fig. 5. The spectral component Fig. 5b is identical with the difference spectrum between all-*trans* T_1 and 9-*cis* S_0 ($a_1 > 0$, $a_3 < 0$) with no contribution from all-*trans* S_0 ($a_2 = 0$). The temporal profiles Fig. 5d is explained in terms of the very fast (880 ps) rise of all-*trans* T_1 and its subsequent relaxation to all-*trans* S_0. The spectral component Fig. 5a is identical with the difference spectrum between all-*trans* S_0 and 9-*cis* S_0 ($a_2 + a_4 > 0$ and $a_3 + a_5 < 0$) with no contribution from all-*trans* T_1 ($a_4 = 0$). The kinetics in Fig. 5c indicates that all-*trans* S_0 is formed at the expense of 9-*cis* S_0.

3.3. Photoisomerization mechanism

The intensity of the 9-*cis* S_0 band at 1144 cm^{-1} (Fig. 2a) decreases at the rate of 5 μs, which is the same rate as that of the decrease of the all-*trans* T_1 bands at 1184 cm^{-1} (Fig. 2c) and 1600 cm^{-1} (Fig. 2d). This fact indicates that a reaction pathway exists that consumes 9-*cis* S_0 by the interaction with all-*trans* T_1. The SVD analysis has shown that all-*trans* S_0 is formed at the expense of 9-*cis* S_0. These two results indicate that the 9-*cis* to all-*trans* isomerization occurs through the interaction between all-*trans* T_1 and 9-*cis* S_0;

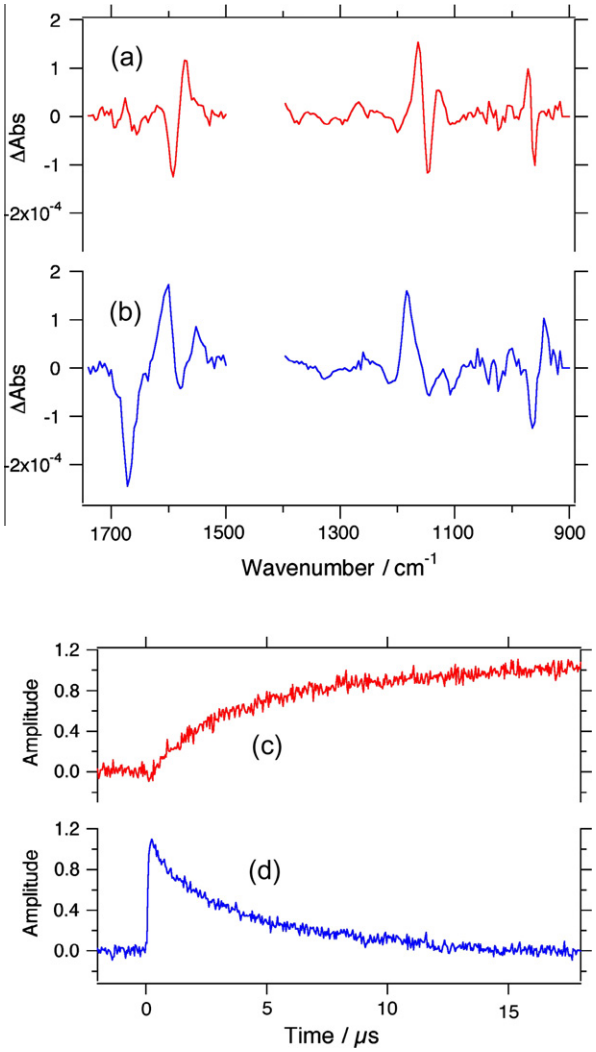

Fig. 5. Retrieved temporal (a, b) and spectral (c, d) components.

all-*trans* T_1 + 9-*cis* S_0 → 9-*cis* T_1 + all-*trans* S_0

→ all-*trans* T_1 + all-*trans* S_0.

All-*trans* T_1 is quenched by 9-*cis* S_0 and 9-*cis* T_1 and all-*trans* S_0 are formed. The 9-*cis* T_1 then isomerizes to all-*trans* T_1 with the time constant of 880 ps [8]. The 9-*cis* T_1 lifetime is too short to be detected with the present nanosecond time-resolved infrared experiment. All-*trans*-T_1 is thus reproduced after reacting with 9-*cis* S_0 with a net isomerization from 9-*cis* S_0 to all-*trans* S_0. The reproduced all-*trans*-T_1 can start another reaction with 9-*cis* S_0. This quantum chain process was suggested for *cis–trans* isomerization of retinal from the very large photoisomerization quantum yields [4,13,14]. To the best of our knowledge, the present time-resolved infrared study is the first direct observation of this quantum chain process.

The spectrum in Fig 5b contains only those of all-*trans* T_1 and 9-*cis* S_0, though Eq. (5) indicates that it can also contain the spectrum all-*trans* S_0. The negligible contribution of all-*trans* S_0 ($a_2 = 0$) indicates that there is no instantaneous rise of all-*trans* S_0 and that the isomerization pathway that includes the instantaneous formation of all-*trans* S_0 from the 9-*cis* excited singlet state is minor, if possible at all. The photoisomerization of 9-*cis* to all-*trans* occurs predominantly on the excited triplet potential surface and not on the excited singlet state.

4. Conclusions

Two distinct pathways have been found for the photoisomerization of 9-*cis* retinal. One is the triplet pathway in the picosecond regime. Another takes place in the microsecond time regime through the energy transfer between all-*trans* T_1 and 9-*cis* S_0. The latter includes the quantum chain process in which all-*trans* T_1 is repeatedly reproduced with net isomerization of 9-*cis* S_0 to all-*trans* S_0.

References

[1] M. Ottolenghi, Adv. Photochem. 12 (1980) 97.
[2] W.H. Wadel, K. Chihara, J. Am. Chem. Soc. 103 (1981) 7389.
[3] R.S. Becker, Photochem. Photobiol. 48 (1988) 369.
[4] S. Ganapathy, R.S.H. Liu, J. Am. Chem. Soc. 114 (1992) 3459.
[5] J. Saltiel, J. D'Agostino, E.D. Magarity, L. Metts, K.R. Neuberger, M. Wrighton, O.C. Zafirou, Org. Photochem. 3 (1971) 1.
[6] H. Hamaguchi, H. Okamoto, M. Tasumi, Y. Mukai, Y. Koyama, Chem. Phys. Lett. 107 (1984) 355.
[7] Y. Hirata, N. Mataga, Y. Mukai, Y. Koyama, Chem. Phys. Lett. 134 (1987) 166.
[8] T. Tahara, B.N. Toleutaev, H.-o. Hamaguchi, J. Chem. Phys. 100 (1994) 786.
[9] S. Yamaguchi, H. Hamaguchi, Chem. Phys. Lett. 287 (1998) 694.
[10] T. Yuzawa, H. Hamaguchi, J. Mol. Struct. 352/353 (1995) 489.
[11] S. Yamaguchi, H. Hamaguchi, J. Mol. Struct. 379 (1995) 87.
[12] S. Yamaguchi, H. Hamaguchi, J. Chem. Phys. 109 (1998) 1397–1408.
[13] Y. Mukai, H. Hashimoto, Y. Koyama, J. Phys. Chem. 94 (1990) 4042.
[14] S. Ganapathy, A. Trehan, R.S.H. Liu, J. Chem. Soc. Chem. Commun. 1990 (1990) 199.
[15] K. Iwata, H. Hamaguchi, Appl. Spectrosc. 44 (1990) 1431–1437.
[16] T. Yuzawa, C. Kato, M.W. George, H. Hamaguchi, Appl. Spectrosc. 48 (1994) 684.
[17] M. Hashimoto, T. Yuzawa, C. Kato, K. Iwata, H. Hamaguchi, in: J.M. Chalmers, P.R. Griffiths (Eds.), Handbook of Vibrational Spectroscopy, John Wiley and Sons Ltd., Chichester, 2002, pp. 666–676.